Separation of coexisting dynamical regimes in multistate intermittency based on wavelet spectrum energies in an erbium-doped fiber laser

Alexander E. Hramov, Alexey A. Koronovskii, Olga I. Moskalenko, and Maksim O. Zhuravlev
Saratov State University, Astrakhanskaya, 83, Saratov 410012, Russia
and Saratov State Technical University, Politehnicheskaya, 77, Saratov 410054, Russia

Rider Jaimes-Reategui
Universidad de Guadalajara, Centro Universitario de los Lagos, Enrique Díaz de León 1144, Paseos de la Montaña, 47460, Lagos de Moreno, Jalisco, Mexico

Alexander N. Pisarchik
Center for Biomedical Technology, Technical University of Madrid, Campus Montegancedo, 28223 Pozuelo de Alarcon, Madrid, Spain
and Centro de Investigaciones en Optica, Loma del Bosque 115, Lomas del Campestre, 37150 Leon, Guanajuato, Mexico
(Received 13 October 2015; revised manuscript received 3 May 2016; published 23 May 2016)

We propose a method for the detection and localization of different types of coexisting oscillatory regimes that alternate with each other leading to multistate intermittency. Our approach is based on consideration of wavelet spectrum energies. The proposed technique is tested in an erbium-doped fiber laser with four coexisting periodic orbits, where external noise induces intermittent switches between the coexisting states. Statistical characteristics of multistate intermittency, such as the mean duration of the phases for every oscillation type, are examined with the help of the developed method. We demonstrate strong advantages of the proposed technique over previously used amplitude methods.

DOI: 10.1103/PhysRevE.93.052218

I. INTRODUCTION

The irregular alternation of two different regimes in time, while all system parameters are fixed, has been observed and studied intensively in many dynamical systems, from electrical circuits [1] and lasers [2] to immensely complex living objects [3–7]. Such behavior was first studied by Pomeau and Manneville [8] in the Lorenz model with alternation of apparently periodic and chaotic regimes, and it was called "intermittency." Later, the same term was used to describe irregular alternation between two different forms of chaotic motion, so-called crisis-induced intermittency [9]. According to the mechanisms resulting in intermittent dynamics and statistic properties of two different types of behavior (traditionally called laminar and turbulent phases), various types of intermittency are distinguished, such as type I–III intermittency [10,11], eyelet intermittency [12–16], ring intermittency [17], and on-off intermittency [18–22]. Each of these types of intermittency is characterized by its own dependence of the mean laminar phase length on the criticality parameter and by the type of laminar phase length distribution observed for fixed parameter values.

Recently, the notion of intermittency was extended to multistable systems (multistate intermittency) manifested as the alternation between coexisting periodic or chaotic behaviors regardless of the form of motion [23,24]. In bistable and multistable dynamical systems, irregular switches between coexisting states can be induced by noise resulting in so-called noise-induced intermittency or noise-induced attractor hopping [25–28]. The switch between two states (two-state intermittency) was studied by Lai and Grebogi [29] and later demonstrated in laser experiments [30]. In the literature, both notions, namely attractor hopping and multistate intermittency, are used to refer to this kind of behavior [27,31]. Although the name may be a subject of discussion, in our opinion the term "multistate intermittency" more accurately reflects the intermittent character of this kind of dynamics in systems with coexisting attractors.

In conjunction with conventional types of intermittency, more sophisticated types were observed. Parameter fluctuations and external noise may significantly change the characteristic properties of intermittent behavior [32–34]. Remarkably, the difference may be so great that under certain circumstances the same type of intermittency can be classified into two completely different dynamical regimes [35]. Furthermore, two or more different intermittency types may alternate with each other, resulting in the emergence of a very complex behavior known as *intermittency of intermittencies* [36]. Obviously, all these sophisticated types of intermittent behavior create additional difficulties in classification and characterization of an observed type of intermittency. The most unrevealed problem seems to arise when we deal with a system with multiple (three or more) coexisting attractors in which additional noise induces intermittent switches between different dynamical regimes. In this case, researchers face the problem associated not only with regularities in the residence time distributions, but also with separation of time intervals belonging to particular dynamical regimes.

Typically, when only two different dynamical regimes are involved in intermittent dynamics, they are usually distinguished in time series using an amplitude criterion. When a typical value of the variable characterizing the system state in one regime (say, regime A) exceeds considerably the value of the corresponding variable of another alternating regime (say, regime B), the difference can be used to distinguish time intervals associated with distinct coexisting regimes. In this case, the threshold value Δ is introduced in such a way that when the dynamical variable x is below this threshold ($x < \Delta$)

the system is in regime A, whereas above the threshold ($x > \Delta$) it is in regime B. Although direct application of this approach yields acceptable results in only a limited number of systems, additional transformation of the system variables makes the amplitude criterion practically a universal tool suitable for a broad range of dynamical systems. Different variations of the amplitude criterion were applied successfully to examine intermittent lag synchronization [21,22,37], intermittent generalized synchronization [38], intermittent phase synchronization [39], etc.

In certain cases, specific operations are required before the application of the amplitude criterion. Since the alternating oscillatory regimes may be characterized by different dominant frequencies, the amplitude criterion can be used to analyze time series of highly complex systems, such as the brain, together with consideration of the system behavior in a certain preliminary defined time-scale range. To examine the dynamical variable $x(t)$ in the time-scale range $s \in [s_l, s_h]$, the integral energy of the wavelet spectrum associated with this range can be calculated as

$$w(t) = \int_{s_l}^{s_h} |W(s,t)|^2 \, ds, \tag{1}$$

where $W(s,t)$ is the complex wavelet surface defined with the help of the continuous wavelet transform

$$W(s,t_0) = \frac{1}{\sqrt{s}} \int_{-\infty}^{+\infty} x(t) \psi^* \left(\frac{t - t_0}{s} \right) dt \tag{2}$$

with the complex Morlet mother wavelet

$$\psi(\eta) = \frac{1}{\sqrt[4]{\pi}} \exp(j\Omega_0 \eta) \exp\left(\frac{-\eta^2}{2} \right). \tag{3}$$

The symbol "$*$" in Eq. (2) denotes complex conjugation. The parameter value $\Omega_0 = 2\pi$ is typically used to provide the relation $s \approx 1/f$ between the time scale s, where the examination is carried out, and the corresponding frequency f of the Fourier transformation [40]. After the calculation of the time dependence of the wavelet spectrum energy Eq. (1) in the considered time-scale range $[s_l, s_h]$, the amplitude criterion $w(t) > \Delta_s$ can be used again to separate the time intervals associated with the alternating regimes. This technique has been used successfully to study intermittency in brain dynamics, where different types of intermittent behavior take place, e.g., those involving spike-wave discharges manifested themselves as electroencephalographic hallmarks of absence epilepsy, sleep spindles, 5–9 Hz oscillations, and background activity [40]. Remarkably, the described approach based on the continuous wavelet transform and the amplitude criterion aims to detect and localize certain patterns of oscillatory dynamics, going far beyond the problem of studying intermittency, and it may also be used separately in advanced brain research.

The efficient technique developed for detection and localization of coexisting regimes in intermittent time series is, in fact, a solid basis promoting considerable success in understanding the core mechanisms and main regularities of the intermittency phenomenon. The basic regularities of more complicated kinds of intermittency, when three or more dynamical regimes are involved, are far from clear. The task of identifying time intervals corresponding to each regime in such complicated time series remains an unsolved problem.

In the present work, as an example and without loss of generality, we consider an erbium-doped fiber laser (EDFL), which is known [2,28] to exhibit the coexistence of multiple attractors, where noise can induce multistate intermittency consisting in irregular alternations between four different periodic regimes, each with its own characteristic amplitude and frequency [23,28]. To analyze this complex type of intermittent behavior, we propose the method of time-interval localization corresponding to particular dynamical regimes. Using the developed method, we reveal the main features of this noise-induced multistate intermittency.

The rest of the paper is organized as follows. In Sec. II, we describe the theoretical model of the EDFL. The core idea, namely the algorithm of the method implementation, and the results of its application are given in Sec. III. In the same section, we compare the efficiency of the proposed method with that of the amplitude method that has previously been used [23,28] to study the intermittent behavior in the same laser. The results of careful consideration of the noise-induced multistate intermittency in the EDFL are discussed in Sec. IV. Finally, comments and remarks are given in Sec. V.

II. MODEL OF THE ERBIUM-DOPED FIBER LASER

The dynamics of the EDFL is described by the following rate-equation model [2]:

$$\begin{aligned} \frac{dx}{dt} &= \frac{2L}{T_r} x\{r_w \alpha_0 [N(\xi_1 - \xi_2) - 1] - \alpha_{\text{th}}\} + P_{\text{sp}}, \\ \frac{dy}{dt} &= -\frac{\sigma_{12} r_w x}{\pi r_0^2}(y\xi_1 - 1) - \frac{x}{\tau} + P_{\text{pump}}, \end{aligned} \tag{4}$$

where x is the intracavity laser power, $y = \frac{1}{n_0 L} \int_0^L N_2(z) dz$ is the averaged (over the active fiber length L) population of the upper lasing level, N_2 is the upper-level population at the z coordinate, n_0 is the refractive index of a "cold" erbium-doped fiber core, and ξ_1 and ξ_2 are parameters defined by the relationship between cross sections of ground-state absorption (σ_{12}), return stimulated transition (σ_{21}), and excited-state absorption (σ_{23}). T_r is the photon intracavity round-trip time, α_0 is the small-signal absorption of the erbium fiber at the laser wavelength, α_{th} accounts for the intracavity losses on the threshold, τ is the lifetime of erbium ions in the excited state, r_0 is the fiber core radius, w_0 is the radius of the fundamental fiber mode, and r_w is the factor that conveys the match between the laser fundamental mode and erbium-doped core volumes inside the active fiber. The spontaneous emission into the fundamental laser mode is derived as

$$P_{\text{sp}} = y \frac{10^{-3}}{\tau T_r} \left(\frac{\lambda_g}{w_0} \right)^2 \frac{r_0^2 \alpha_0 L}{4\pi^2 \sigma_{12}}, \tag{5}$$

where λ_g is the laser wavelength. The pump power is expressed as

$$P_{\text{pump}} = P_p \frac{1 - \exp[-\alpha_0 \beta L(1 - y)]}{N_0 \pi r_0^2 L}, \tag{6}$$

where P_p is the pump power at the fiber entrance and β is a dimensionless coefficient. We explore the following parameter

values: $L = 0.88$ m, $T_r = 8.7$ ns, $r_w = 0.308$, $\alpha_0 = 40$ m^{-1}, $\xi_1 = 2$, $\xi_2 = 0.4$, $\alpha_{\text{th}} = 3.92 \times 10^{-2}$, $\sigma_{12} = 2.3 \times 10^{-17}$ m^2, $r_0 = 2.7 \times 10^{-6}$ m, $\tau = 10^{-2}$ s, $\lambda_g = 1.65 \times 10^{-6}$ m, $w_0 = 3.5 \times 10^{-6}$ m, $\beta = 0.5$, and $N_0 = 5.4 \times 10^{25}$ m^{-3}, which correspond to the real experimental conditions that will be described in the following section.

Under harmonic modulation $m_d \sin(2\pi f_d t)$ applied to the diode pump current as

$$P_p = p[1 - m_d \sin(2\pi f_d t)] \tag{7}$$

within a certain range of driving amplitude $m_d \in (0.95, 1.0]$ and driving frequency f_d, the EDFL Eq. (4) exhibits the coexistence of up to four periodic orbits A_i ($i = 1,3,4,5$) with frequencies $f_i = f_d/i$ corresponding to the periods 1, 3, 4, and 5. In Eq. (7), p is the pump power.

When both harmonic and random modulations are added to the pump current as [23]

$$P_p = p[1 - m_d \sin(2\pi f_d t) + \eta G(\zeta, f_n)], \tag{8}$$

the phase-space trajectory alternatively visits different attracting domains of the phase space leading to multistate intermittency, i.e., the laser switches between different periodic regimes, as seen in the time series in Figs. 1(a) and 3(a). In Eq. (8), η is the noise amplitude and $G(\zeta, f_n)$ is the zero-mean noise function of a random number $\zeta \in [-1,1]$ and noise low-pass cutoff frequency f_n (white noise is filtered with a fifth-order discrete low-pass Butterworth filter in LABVIEW 8.5). The parameters of stochastic modulation, f_n and η, determine the number of coexisting states and the preference for each of the periodic orbits involved in multistate intermittency. In this work, we fix the driving frequency to $f_d = 80$ kHz and set the amplitude of harmonic modulation to $m_d = 0.95$. In our previous paper [23], we studied the dependence of the probability to detect different regimes on the noise bandwidth and found that the most diverse dynamics occurs when noise is filtered at $f_n = 30$ kHz. Therefore, in the present work we use exactly the same value of f_n.

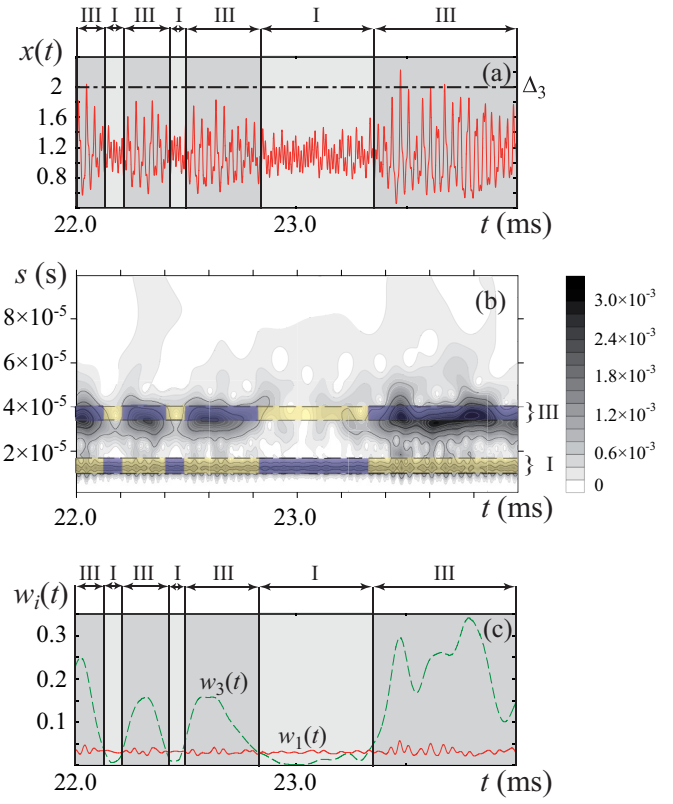

FIG. 1. Dynamics of EDFL demonstrating noise-induced multistate intermittency. For noise intensity $\eta = 0.23$, two different dynamical regimes (namely, period-1 and period-3) alternate: (a) time series of $x(t)$, (b) wavelet surface $|W(s,t)|$, and (c) dependence of wavelet spectrum energies $w_{1,3}(t)$ on time t. The Roman numerals show the regimes with different oscillation periods. The threshold Δ_3 used for the amplitude criterion is shown by the dot-dashed line in (a). The characteristic time scales for these regimes, $s_{1,3} \pm \Delta s$, are marked by the dashed lines in (b).

III. METHOD FOR REGIME DETECTION

The method for detection and localization of different dynamical regimes alternating with each other is based on the continuous wavelet transform Eq. (2) with the Morlet mother wavelet function Eq. (3). Since each of the coexisting limit cycles of period-i ($i = 1,3,4,5$) is characterized by its own frequency f_i, the maximum energy $|W(s,t_0)|^2$ of the wavelet spectrum $W(s,t_0)$ is observed in the time scale $s_i \approx 1/f_i$ corresponding to the dynamical regime realized at the moment of time t_0.

The core idea of the proposed method is illustrated in Fig. 1, where the fragment of the time series [Fig. 1(a)] generated by the EDFL model Eq. (4) with the noise intensity value $\eta = 0.23$ is analyzed. For the given values of the control parameters, only two dynamical regimes with the main frequencies f_1 and f_3 alternate with each other.

The wavelet surface $|W(s,t)|$ shown in Fig. 1(b) illustrates the process of sudden switches between the coexisting oscillatory regimes that can be easily monitored with the help of the tracking of the wavelet spectrum energy in certain time scales s_i corresponding to the main frequencies f_i of the alternating regimes. In other words, the level of the wavelet energy in the corresponding time scale may be used as a regime marker. To detect which type of dynamical regime takes place at time t_0, one has to compare the wavelet spectrum energies $|W(s_i,t_0)|^2$ for each regime. The wavelet surface $|W(s,t)|$ [Fig. 1(b)] corresponding to the considered fragment of the time series and the time series itself [Fig. 1(a)] makes evident the time intervals where the dynamical regimes with frequencies f_1 and f_3 take place.

Although the continuous wavelet transform is known to neutralize the effect of noise at the main frequencies [40], allowing us to use this method for filtering noisy signals, the main frequencies of the alternating dynamical regimes of the EDFL in the presence of external noise still fluctuate [Fig. 1(b)], and therefore the consideration of the integral wavelet spectrum energy within rather narrow time-scale intervals $s_i - \Delta s \leqslant s \leqslant s_i + \Delta s$ [by analogy with Eq. (1)],

$$w_i(t) = \frac{1}{2\Delta s} \int_{s_i - \Delta s}^{s_i + \Delta s} \frac{|W(s,t)|^2}{s}\, ds, \tag{9}$$

seems to be more appropriate. The factor $1/s$ allows a direct comparison of the energies of the competitive regimes, because for the same amplitude of the harmonic signal $A\sin(2\pi t/s)$ the wavelet spectrum energy is known to increase quadratically as the time scale s grows [40]. The dynamical regime, which takes place at a certain moment of time t_0, is detected with the help of the largest wavelet spectrum energy $w_i(t_0)$.

The approach described above is used to separate the coexisting dynamical regimes shown in Fig. 1(c). One can see that within the time intervals corresponding to the existence of the dynamical regime with the driving frequency $f_1 = f_d = 80$ kHz, the wavelet spectrum energy $w_1(t)$ prevails over $w_3(t)$ and vice versa [Fig. 1(c)]. Note also that the value of $w_1(t)$ changes over time insufficiently, i.e., its value remains practically the same even within time intervals when the regime with the characteristic frequency f_3 takes place. This aspect is explained by the fact that the driving frequency f_d always exists regardless of the dynamical regime released in the system. Therefore, the modulation frequency f_d superimposes on the system dynamics and becomes reflected into the wavelet spectrum [41]. Since the amplitude of the modulation is constant, the value of $w_1(t)$ obtained for the time-scale range corresponding to the frequency f_1 changes insufficiently [see Fig. 1(c)]. The moments of time when the wavelet energies $w_1(t)$ and $w_3(t)$ coincide are supposed to correspond to switches between the competitive regimes. More precisely, these switches are not instantaneous, however we neglect their duration because they are too short in comparison with the duration of the alternating regimes.

As we already mentioned in the Introduction, multistate intermittency in the EDFL with four coexisting states was previously studied using the amplitude method [23,28], however the technique of wavelet spectrum energies was not used. Let us demonstrate how it works. To separate coexisting period-1, period-3, period-4, and period-5 regimes, three threshold values, $\Delta_3 = 2$, $\Delta_4 = 6$, and $\Delta_5 = 12$, are chosen empirically. When the oscillation amplitude does not exceed the threshold value for the period 3 (Δ_3), the basic period-1 oscillation regime with the main frequency f_1 is supposed to take place. The oscillations with the amplitudes being within the range $[\Delta_3, \Delta_4]$ are considered to belong to the period-3 dynamical regime characterized by the main frequency $f_3 = 30$ kHz. Similarly, when the amplitude of the oscillations occurs within the interval $[\Delta_4, \Delta_5]$, the observed regime is interpreted as period-4 with the main frequency f_4. Finally, the oscillations with the amplitudes exceeding the highest threshold value Δ_5 are supposed to belong to the period-5 regime with the main frequency f_5.

Next, we will show that the amplitude method can only be used for qualitative estimations, but not for precise quantitative analysis. To illustrate this statement, we compare the results obtained using the amplitude method with the results obtained using the proposed approach. For this purpose, we plot in Fig. 1(a) the corresponding threshold Δ_3 by the dot-dashed line. One can see that even if only two oscillatory regimes are involved in intermittency, i.e., even if we deal with the simplest manifestation of the multistate intermittency (two-state intermittency), the amplitude method yields a very rough estimation. Indeed, as clearly seen from the time series in Fig. 1(a), within the time interval $22.2 \leqslant t \leqslant 22.4$ ms, the amplitude criterion testifies to the presence of the dynamical regime with the frequency f_1, while the oscillations with the main frequency f_3 take place [compare the time series in Fig. 1(a) and the wavelet surface in Fig. 1(b)] because inside this interval of length $T = 0.2$ ms six oscillation periods ($N \approx 6$) are observed, and therefore the computed oscillation frequency and time scale are $f = N/T \approx 30.0$ kHz $= f_3$ and $s \approx 3.3 \times 10^{-2}$ ms, respectively. Exactly the same situation occurs for other time intervals where the period-3 regime takes place. The mean residence times $\langle l_1 \rangle$ and $\langle l_3 \rangle$ for the regimes with the main frequencies f_1 and f_3 obtained with the help of the proposed method are $\langle l_1 \rangle = 0.108$ ms and $\langle l_3 \rangle = 0.793$ ms, which is in good agreement with Fig. 1. On the contrary, the mean residence times $\langle \hat{l}_1 \rangle = 6.410$ ms and $\langle \hat{l}_3 \rangle = 0.003$ ms found by means of the amplitude method completely contradict the observed dynamics. This allows us to conclude that the method based on the comparison of the wavelet spectrum energies $w_i(t)$ [Fig. 1(c)] yields correct results where the amplitude method fails.

Taking into account the above aspect and using the proposed method of the regime detection accordingly, we analyze the time series corresponding to the intermittent switches between several dynamical regimes (Figs. 2 and 3). Such intermittent dynamics is observed in the EDFL for the control parameters $\eta = 0.47$ and 0.97.

One can see from the time series $x(t)$ shown in Figs. 2(a) and 3(a) that within the considered time intervals, three different dynamical regimes (period-1, -2, and -4 in Fig. 2 and period-3, -4, and -5 in Fig. 3) alternate with each other. An increase in the noise intensity results in a modification of the oscillation shape because the pulses become very sharp. The abrupt oscillation fronts generate a rapid (but very short) growth of the wavelet energy $|W(s,t_0)|^2$ in a broad range of time scales, especially on the short ones [Fig. 3(b)]. As a consequence, the considered wavelet spectrum energy within the narrow time-scale interval corresponding to the small time scale, $w_1(t)$, starts showing surges in the amplitude coinciding with the oscillation fronts [compare Figs. 3(b) and 3(c)]. Importantly, although during these spikes the wavelet energy $w_1(t)$ can exceed the analogous values $w_i(t)$ corresponding to other regimes (e.g., time interval $5.36 \leqslant t \leqslant 5.70$ ms in Fig. 3), these events are fulminant and do not contain the period-1 dynamical regime with frequency f_1. Therefore, to avoid the false detection of switches between different regimes, one has to exclude from consideration short time intervals whose length is about one or two oscillation periods.

Again, as in the case of two coexisting regimes shown in Fig. 1, we can conclude that the proposed method based on the comparison of the wavelet spectrum energies $w_i(t)$ yields correct results and surpasses the amplitude method used in earlier works. Thus, the proposed method, which is aimed at detecting and localizing different dynamical regimes alternating with each other in a complex nonlinear system, may be considered as a powerful tool to examine multistate intermittent behavior. In particular, this approach is applied to the noisy EDFL. The amplitude method used before is, in turn, less accurate and can only be used for qualitative estimations, while it is unfit for precise quantitative measurements.

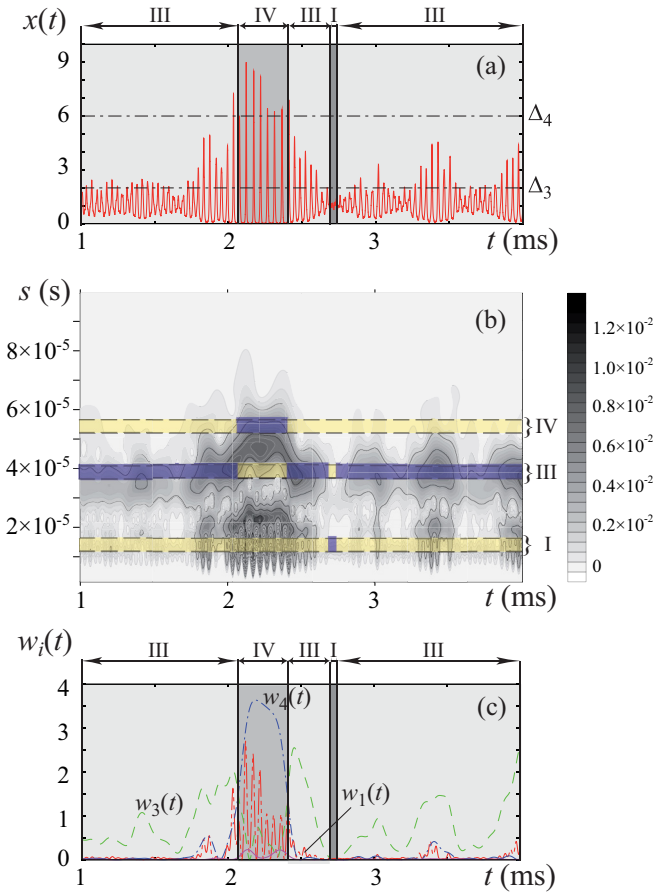

FIG. 2. Illustration of the efficiency of the proposed method for noise intensity $\eta = 0.47$ when three dynamical regimes, period-1, period-3, and period-4 with frequencies f_1, f_3, and f_4, alternate with each other. (a) Fragment of analyzed time series $x(t)$, (b) wavelet surface $W(s,t)$, and (c) dependence of wavelet spectrum energies $w_{1,3,4}(t)$ on time t. The thresholds Δ_3 and Δ_4 used for the amplitude criterion are shown by the dashed lines.

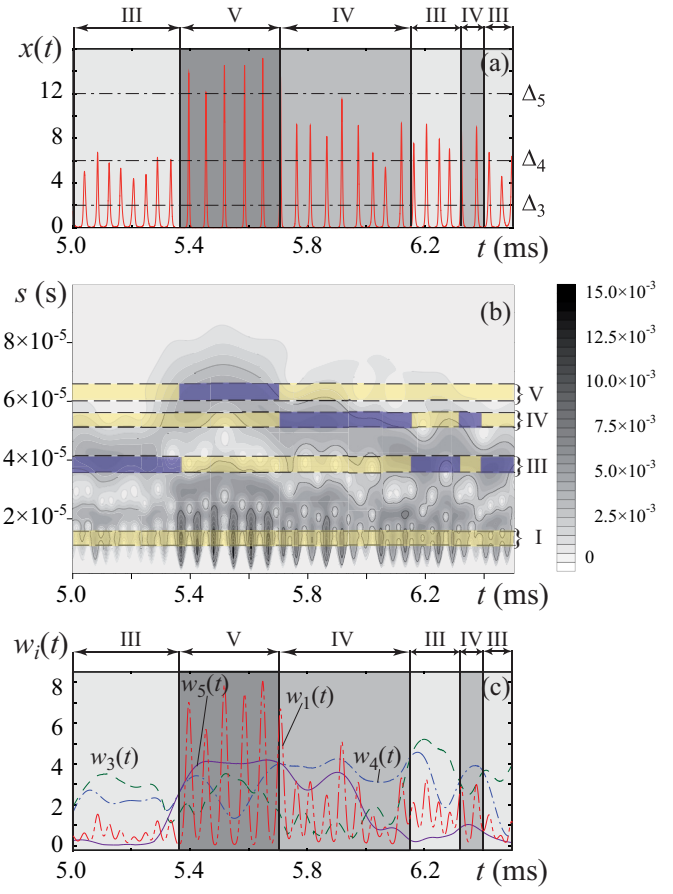

FIG. 3. Illustration of the efficiency of the proposed method for noise intensity $\eta = 0.97$ when three dynamical regimes, period-3, period-4, and period-5 with frequencies f_3, f_4, and f_5, alternate with each other. (a) Fragment of analyzed time series $x(t)$, (b) wavelet surface $W(s,t)$, and (c) dependence of wavelet spectrum energies $w_{3,4,5}(t)$ on time t. The thresholds Δ_3, Δ_4, and Δ_5 used for the amplitude criterion are shown by the dashed lines.

IV. MULTISTATE INTERMITTENCY

Since the proposed approach allows the localization of precise time intervals associated with a particular state in multistate intermittency, it makes possible a careful study of the statistical characteristics of such intricate behavior. The EDFL dynamics and main features of intermittency are known to be determined by the noise intensity, therefore it is important to consider the system behavior in a wide range of noise intensities.

To characterize the domination of a particular dynamical regime in the time series at a fixed value of the noise intensity, we calculate the dependence of the probability for the emergence of a certain dynamical regime P_i ($i = 1,3,4,5$) on the noise intensity η (Fig. 4) defined as

$$P_i = \lim_{L\to+\infty} L_i/L, \tag{10}$$

where L_i is the sum of lengths of all the time intervals corresponding to the ith dynamical regime in the examined time series with length $L = L_1 + L_3 + L_4 + L_5$. In our study,

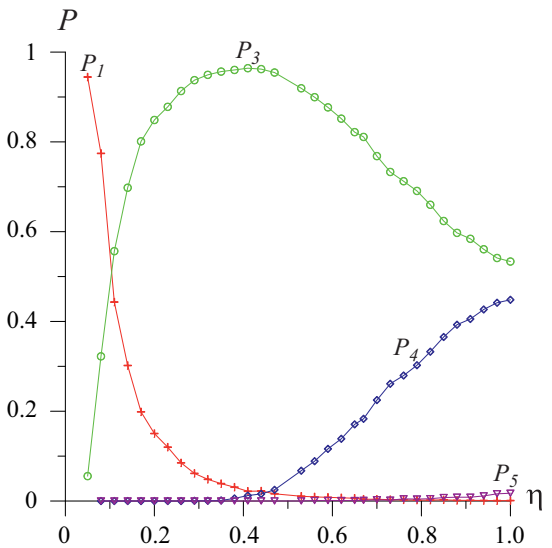

FIG. 4. Probability to detect dynamical regime P_i ($i = 1,3,4,5$) vs noise intensity η.

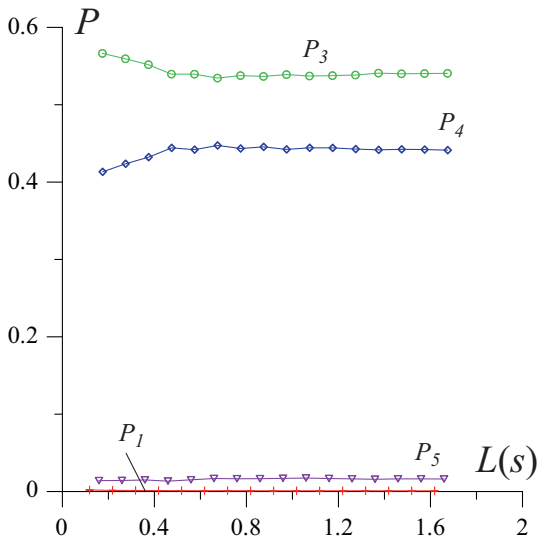

FIG. 5. Probability to detect dynamical regime P_i ($i = 1,3,4,5$) as a function of time-series length L for every regime obtained for noise intensity $\eta = 0.97$.

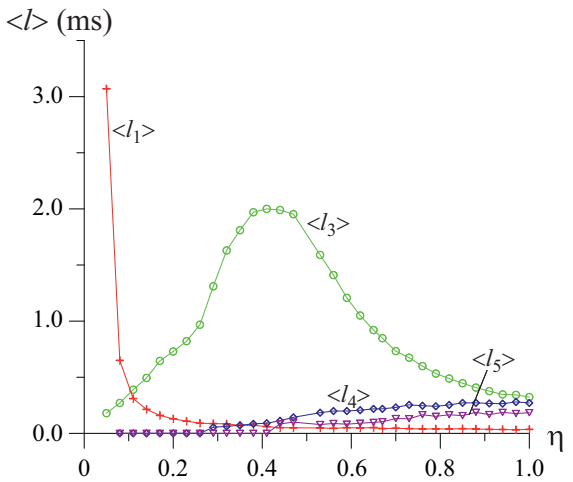

FIG. 6. Mean residence time $\langle l \rangle$ vs noise intensity η for every detected regime.

we use the time series with length $L = 1.68$ s for each value of the noise intensity η.

Obviously, for the time series obtained both experimentally and numerically, the values of P_i can only be found for the finite-length time series, whereas in Eq. (10) the length of the time series, L, tends to infinity, i.e., the probability to detect the ith dynamical regime is defined for the infinite time series. As a consequence, in the experimental observations and numerical simulations, the probability to detect the ith dynamical regime, P_i, is always defined with a certain accuracy δ_i, and therefore one needs to control the length of the time series, L, to be sure that the obtained results are correct. Figure 5 shows the dependencies of the probability values for different dynamical regimes obtained for the noise intensity $\eta = 0.97$ on the time-series length L. One can see that for the small lengths ($L < 0.5$), a change in L results in notable changes in the probability P_i, whereas for the larger lengths the probability remains practically constant. For the time-series length $L = L_0 = 1.68$ s used in the present study and the noise intensity $\eta = 0.97$, the relative error δ_i is less than 1%, and therefore the time-series length L_0 allows for a quantitative characterization of the system dynamics with very high accuracy. Similar estimations of the relative error values are obtained for other noise intensities η as well as for other quantities used in our work to characterize multistate intermittency (see Figs. 6 and 7).

The probability of detecting the dynamical regime with the main frequency f_i shown in Fig. 4 depends crucially on the noise intensity η; the character of this dependence is different for each regime. For small values of the noise intensity η, the most typical regime is characterized by the frequency f_1 (its probability is more than 90%). The second dynamical regime, which can also be observed for small noise intensity (although its probability is low), is the period-3 regime, while the probability for the regimes with the main frequencies f_4 and f_5 is equal to zero. As the noise intensity η increases, the probability to detect the period-1 regime rapidly decreases, while the analogous probability for the period-3 regime grows (Fig. 4). Starting from the middle level of the noise intensity, the other two dynamical regimes with the main frequencies f_4 and f_5 spring up in the time series with a relatively small probability to be observed. Nevertheless, the higher the noise intensity η, the larger is the probability for the period-4 regime, whereas the probability to detect the regime with the main frequency f_5 remains small. Remarkably, the period-1 regime being dominant for small noise intensities is practically destroyed by stronger noise, and the probability P_1 tends to be close to zero for $\eta > 0.7$.

Another important characteristic of the intermittent behavior is the dependence of the mean residence time on the control parameter (in our case, on the noise intensity η). Figure 6 shows the dependencies of the mean residence time on the noise intensity for all coexisting dynamical regimes observed in the EDFL. Since the mean residence time correlates with the probability for the detection of a dynamical regime, the curves shown in Fig. 6 are similar to the probability functions in Fig. 4. The short residence times of all regimes observed for large values of η are explained by the frequent switches between modes, caused by the large noise intensity.

One of the most important and informative characteristics of the intermittent behavior for a fixed control parameter is the residence time distribution. Therefore, here we calculate the probability distribution of the duration of every dynamical regime for three different values of the noise intensity, namely $\eta = 0.23$, 0.47, and 0.97, shown in Figs. 1–3. As the noise intensity η increases, the probability distributions for the residence times corresponding to the regimes with frequencies f_i ($i = 1,3,4,5$) change significantly (Fig. 7). Moreover, with a further increase in the noise intensity, the number of time intervals corresponding to the same dynamical regime (say, period-3) is also changed considerably. This can be clearly seen by comparing the distributions for the period-1 regime for $\eta = 0.23$ and 0.97 in Figs. 7(a) and 7(c).

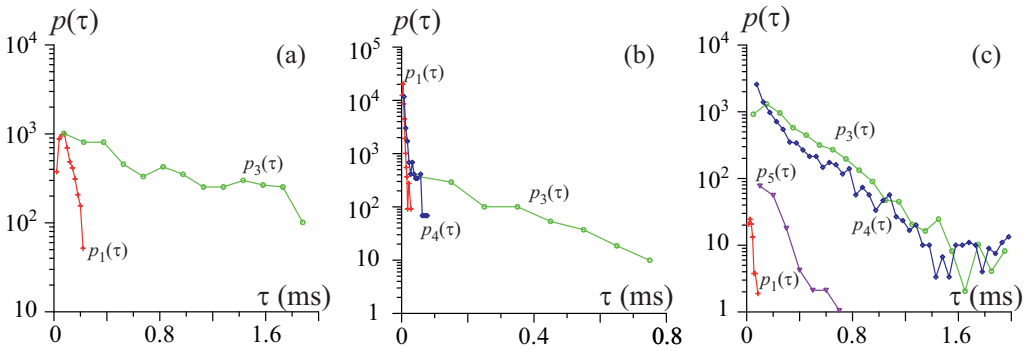

FIG. 7. Probability distributions for lengths of period-1, period-3, period-4, and period-5 dynamical regimes with main frequencies f_1, f_3, f_4, and f_5, respectively, obtained for noise intensity (a) $\eta = 0.23$, (b) $\eta = 0.47$, and (c) $\eta = 0.97$.

V. CONCLUSION

In the present work, we have developed a technique to analyze multistate intermittency. As a prototypical multistable system, we have considered an erbium-doped fiber laser in which noise induces random switches between coexisting periodic orbits. The testing of this method proved to be highly effective for the localization of time intervals corresponding to different dynamical regimes. Using this approach, we have analyzed the main features of noise-induced multistate intermittency in the EDFL. One of the interesting and intricate findings is the sufficient rearrangement of the coexisting regimes observed when the noise intensity varies. In fact, relatively strong noise destroys the most stable dynamical regime and at the same time brings to life completely different states, atypical of the noiseless laser.

It should be noted that the proposed technique requires prior knowledge about coexisting oscillatory regimes. In the considered case of the EDFL, the coexisting dynamical regimes are known from both theoretical and experimental studies of the noiseless EDFL. The notion of frequencies of the coexisting regimes allows the selection of time-scale intervals $s_i - \Delta s \leqslant s \leqslant s_i + \Delta s$ in an optimal way to calculate the wavelet spectrum energy $\omega_i(t)$. Obviously, in many real experimental situations, noise cannot be switched off and therefore internal perturbations (random or chaotic) may mask the coexisting regimes and their main frequencies. This masking can prevent both proper detection of the coexisting regimes and a determination of the maximal meaningful frequency, which should be known *a priori* in order to eliminate fast artifacts, as described in Sec. IV. The colored noise in the system can also cause problems in the detection and separation of coexisting regimes, because some peaks in the noisy Fourier spectrum may be interpreted erroneously as being associated with deterministic components. At the same time, external noise (e.g., detection noise) is not expected practically to have any detrimental effect on the performance of the proposed technique, due to the properties of the continuous wavelet transform [40], except for noise of sufficiently large intensity or color noise, which frequency-matches the main frequency of one of the coexisting regimes. In any case, before application of the proposed approach to the analysis of multistate intermittency, the system dynamics should be examined carefully in order to reveal all of the coexisting regimes and corresponding time-scale ranges.

Finally, we believe that the proposed technique based on wavelet spectrum energies will be helpful in analyzing multistate intermittency in other complex dynamical systems with coexisting oscillatory regimes.

ACKNOWLEDGMENTS

This work has been supported by the Russian Foundation for Basic Research (Grants No. 15-32-20299 and No. 16-32-60078) and Ministry of Education and Science of Russian Federation in the framework of the implementation of state assignment (project 3.59.2014/K). A.E.H. also acknowledges support from the Ministry of Education and Science of Russian Federation in the framework of providing research (Project 931).

[1] I. M. Kyprianidis, M. L. Petrani, J. A. Kalomiros, and A. N. Anagnostopoulos, Phys. Rev. E **52**, 2268 (1995).
[2] A. N. Pisarchik, A. V. Kir'yanov, Y. O. Barmenkov, and R. Jaimes-Reategui, J. Opt. Soc. Am. B **22**, 2107 (2005).
[3] J. L. Perez Velazquez *et al.*, Eur. J. Neurosci. **11**, 2571 (1999).
[4] J. L. Cabrera and J. G. Milton, Phys. Rev. Lett. **89**, 158702 (2002).
[5] C. Park, R. M. Worth, and L. L. Rubchinsky, Phys. Rev. E **83**, 042901 (2011).
[6] P. Gong, A. R. Nikolaev, and C. van Leeuwen, Phys. Rev. E **76**, 011904 (2007).
[7] S. Ahn, C. Park, and L. L. Rubchinsky, Phys. Rev. E **84**, 016201 (2011).
[8] P. Manneville and Y. Pomeau, Phys. Lett. A **75**, 1 (1979).
[9] C. Grebogi, E. Ott, F. J. Romeiras, and J. A. Yorke, Phys. Rev. A **36**, 5365 (1987).
[10] P. Bergé, Y. Pomeau, and C. Vidal, *L'Ordre Dans Le Chaos* (Hermann, Paris, 1988).

[11] M. Dubois, M. A. Rubio, and P. Bergé, Phys. Rev. Lett. **51**, 1446 (1983).
[12] A. S. Pikovsky, M. Zaks, M. G. Rosenblum, G. V. Osipov, and J. Kurths, Chaos **7**, 680 (1997).
[13] K. J. Lee, Y. Kwak, and T. K. Lim, Phys. Rev. Lett. **81**, 321 (1998).
[14] S. Boccaletti, E. Allaria, R. Meucci, and F. T. Arecchi, Phys. Rev. Lett. **89**, 194101 (2002).
[15] E. Rosa, E. Ott, and M. H. Hess, Phys. Rev. Lett. **80**, 1642 (1998).
[16] A. S. Pikovsky, G. V. Osipov, M. G. Rosenblum, M. Zaks, and J. Kurths, Phys. Rev. Lett. **79**, 47 (1997).
[17] A. E. Hramov, A. A. Koronovskii, M. K. Kurovskaya, and S. Boccaletti, Phys. Rev. Lett. **97**, 114101 (2006).
[18] N. Platt, E. A. Spiegel, and C. Tresser, Phys. Rev. Lett. **70**, 279 (1993).
[19] J. F. Heagy, N. Platt, and S. M. Hammel, Phys. Rev. E **49**, 1140 (1994).
[20] M. G. Rosenblum, A. S. Pikovsky, and J. Kurths, Phys. Rev. Lett. **78**, 4193 (1997).
[21] S. Boccaletti and D. L. Valladares, Phys. Rev. E **62**, 7497 (2000).
[22] M. Zhan, G. W. Wei, and C. H. Lai, Phys. Rev. E **65**, 036202 (2002).
[23] A. N. Pisarchik, R. Jaimes-Reategui, R. Sevilla-Escoboza, and G. Huerta-Cuellar, Phys. Rev. E **86**, 056219 (2012).
[24] R. Sevilla-Escoboza, J. M. Buldu, A. N. Pisarchik, S. Boccaletti, and R. Gutierrez, Phys. Rev. E **91**, 032902 (2015).
[25] F. T. Arecchi, R. Badii, and A. Politi, Phys. Rev. A **32**, 402 (1985).
[26] K. Wiesenfeld and P. Hadley, Phys. Rev. Lett. **62**, 1335 (1989).
[27] S. Kraut and U. Feudel, Phys. Rev. E **66**, 015207 (2002).
[28] A. N. Pisarchik, R. Jaimes-Reategui, R. Sevilla-Escoboza, G. Huerta-Cuellar, and M. Taki, Phys. Rev. Lett. **107**, 274101 (2011).
[29] Y. C. Lai and C. Grebogi, Phys. Rev. E **52**, R3313 (1995).
[30] A. N. Pisarchik and V. J. Pinto-Robledo, Phys. Rev. E **66**, 027203 (2002).
[31] G. Huerta-Cuellar, A. N. Pisarchik, and Y. O. Barmenkov, Phys. Rev. E **78**, 035202 (2008).
[32] J. P. Eckmann, L. Thomas, and P. Wittwer, J. Phys. A **14**, 3153 (1981).
[33] W. H. Kye and C. M. Kim, Phys. Rev. E **62**, 6304 (2000).
[34] R. J. Reategui and A. N. Pisarchik, Phys. Rev. E **69**, 067203 (2004).
[35] A. E. Hramov, A. A. Koronovskii, M. K. Kurovskaya, and O. I. Moskalenko, Phys. Lett. A **375**, 1646 (2011).
[36] A. E. Hramov, A. A. Koronovskii, O. I. Moskalenko, M. O. Zhuravlev, V. I. Ponomarenko, and M. D. Prokhorov, Chaos **23**, 033129 (2013).
[37] A. N. Pisarchik and R. Jaimes-Reategui, Phys. Lett. A **338**, 141 (2005).
[38] A. E. Hramov and A. A. Koronovskii, Europhys. Lett. **70**, 169 (2005).
[39] M. Zhuravlev, M. K. Kurovskaya, and O. I. Moskalenko, Tech. Phys. Lett. **36**, 457 (2010).
[40] A. E. Hramov, A. A. Koronovskii, V. A. Makarov, A. N. Pavlov, and E. Sitnikova, *Wavelets in Neuroscience*, Springer Series in Synergetics (Springer, Heidelberg, 2015).
[41] A. E. Hramov, A. A. Koronovskii, V. I. Ponomarenko, and M. D. Prokhorov, Phys. Rev. E **73**, 026208 (2006).